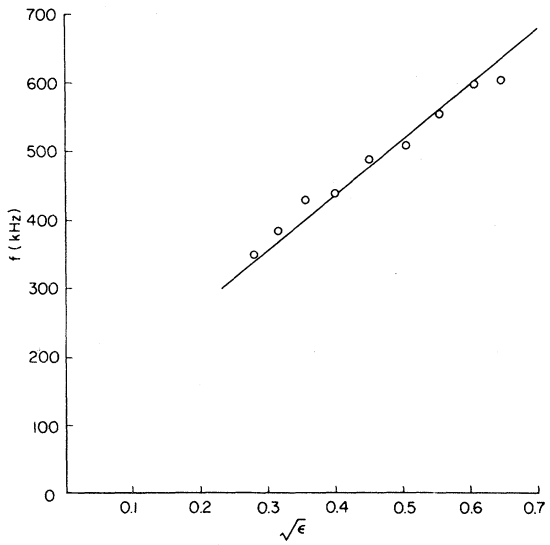

FIG. 4. Frequency of largest-amplitude trapped-electron wave versus $\sqrt{\epsilon}$.

numbers are high: Typically we have measured $m \sim 6$–12. We have measured the fluctuation amplitude, $\tilde{\varphi}_{rms}$, as a function of both radial and axial position. We find that the oscillations are strongly localized radially, with the peak amplitude occurring in the region of minimum η in agreement with theoretical predictions. In the axial direction we observe that $\tilde{\varphi}_{rms}(z)$ is periodic along z in a manner consistent with the assumption that $\tilde{\varphi}_m(z)$ is odd about B_{min}. To confirm the fact that $\tilde{\varphi}_m(z)$ is indeed an odd function, we have taken cross-correlation measurements between probes at fixed axial positions but carefully aligned on the same magnetic field line. These results are also consistent with $\tilde{\varphi}_m(z)$ odd about B_{min}.

We have investigated the mode dependence on ϵ, the trapping-well depth. In Fig. 4 we have plotted the frequency of the primary mode versus $\sqrt{\epsilon}$. We observe that the frequency increases linearly with $\sqrt{\epsilon}$ as predicted by the theory, although the relation is not simply $\omega \propto \sqrt{\epsilon}$, since the curve does not have a zero frequency intercept. The saturated-wave amplitude also exhibits an increase with increasing $\sqrt{\epsilon}$; we observe that $\tilde{\varphi}_{rms}$ increases somewhat faster than linearly with $\sqrt{\epsilon}$.

In summary, we have observed new oscillations in a linear device in the presence of a spatially periodic magnetic field. A comparison of the experimental observations with the theoretical predictions summarized in Table I shows that the observed waves are consistent with the theoretical predictions in virtually all respects. We therefore identify the oscillations as belonging to the trapped-electron-scattering mode.

We thank G. Rewoldt for helpful discussions and for development of the computer code used in the numerical solutions.

*Work supported by the National Science Foundation under Grant No. GK-37979-X.

[1]There have been many papers written on the subject of trapped-particle modes. Probably the best published review paper is B. B. Kadomtsev and O. P. Pogutse, Nucl. Fusion 11, 67 (1971).

[2]B. Coppi and G. Rewoldt, Massachusetts Institute of Technology, Research Laboratory of Electronics, Report No. PRR-749, 1974 (to be published).

[3]B. Coppi, Phys. Rev. Lett. 29, 1076 (1972).

[4]C. W. Horton, Jr., J. D. Callen, and M. N. Rosenbluth, Phys. Fluids 14, 2019 (1971).

Calculated Energy Levels and Optical Absorption in *n*-Type Si Accumulation Layers at Low Temperature

Frank Stern
IBM Thomas J. Watson Research Center, Yorktown Heights, New York 10598
(Received 9 July 1974)

Self-consistent sub-band splittings and inter-sub-band optical matrix elements are calculated for *n*-type accumulation layers at temperatures low enough that the bulk carriers are frozen out. The energy splittings are sensitive to the concentration of *acceptor* impurities in the surface space-charge layer.

Quantum effects in accumulation layers have been studied theoretically by several authors,[1-3] and experimental results have been obtained for InAs,[4] Te,[5,6] PbTe,[7] and Si.[8] This paper gives results of numerical self-consistent calculations for sub-band splittings of accumulation layers in

n-type Si (100) surfaces at low temperatures for which the Fermi level in the bulk lies near the donor level and there are essentially no free carriers in the bulk. It also gives an expression for the optical absorption in the transmission-line configuration used by Kamgar *et al.*[8] and gives numerical results for the matrix element which enters in the absorption coefficient. A noteworthy feature of the low-temperature accumulation-layer case is that the fixed space charge which determines the field at the edge of the accumulation layer is provided by the minority impurities, i.e., by acceptor impurities in n-type Si.

At low temperatures the Fermi level in n-Si is near the energy of the donor level,[9] because there are always expected to be some compensating acceptor impurities present. If a positive electric field is applied across the oxide separating the sample from the gate electrode, negative space charge is induced in the Si and the bands are bent down at the surface. Except for a transition region whose thickness is of the order of a few screening lengths,[10] the donor level in the space-charge layer lies below the Fermi level and is fully occupied by electrons. The space charge then is associated with the acceptors, which are negatively charged. As the nominal conduction-band edge drops below the Fermi level, the electric sub-bands in the resulting potential well can be occupied by electrons and these then contribute to the accumulation-layer space charge.

The low-temperature case I have described is simpler than the more general accumulation-layer case[2] because no allowance need be made for space charge arising from the conduction-band electrons in the bulk. The calculation here does, however, include fixed space charge associated with minority impurities, which was not included in some earlier calculations.[1,3] The present case is computationally equivalent to the case of inversion layers[11] except that the band bending in the fixed-space-charge layer is smaller and that the fixed space charge arises from the minority rather than the majority impurities. Figure 1 shows results for the energies separating the lowest sub-band and the first two excited sub-bands associated with the two lowest valleys for a Si (100) surface. I assumed conduction-band masses of $0.20m$ and $0.916m$, a Fermi level 44 meV below the conduction-band edge in the bulk, and an acceptor concentration of 10^{20} m^{-3}.

I have also calculated sub-band splittings for 10^{19} and 10^{21} acceptors/m^3. The splittings differ from those shown in Fig. 1 by an amount which

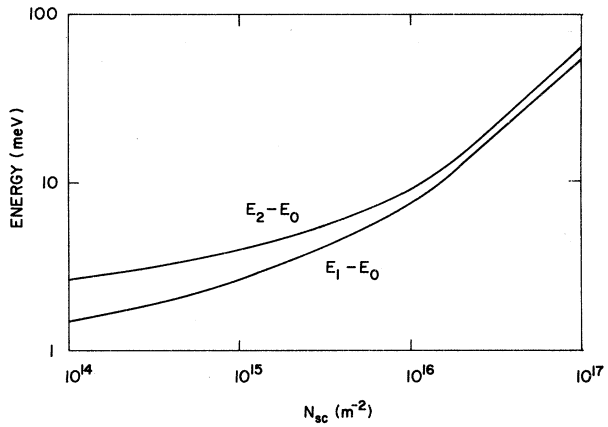

FIG. 1. Energy separation between the lowest sub-band and the first two excited sub-bands arising from the same conduction-band valleys for n-type Si (100) surfaces at 4.2 K, versus the total concentration of accumulation-layer space charges including the fixed space charges associated with acceptor ions. The acceptor concentration is 10^{20} m^{-3} and the Fermi level is assumed to lie 44 meV below the conduction-band edge in the bulk. The bottom of the first excited sub-band crosses the Fermi level near $N_{sc}=4\times10^{16}$ m^{-2}.

is a slowly varying function of the surface space-charge concentration N_{sc}. At $N_{sc}=10^{16}$ m^{-2}, E_{01} and E_{02} must be decreased by 0.3 and 0.8 meV, respectively, relative to the values in Fig. 1 when $N_A=10^{19}$ m^{-3}, and they must be increased by 1.4 and 2.9 meV, respectively, when $N_A=10^{21}$ m^{-3}; $E_{ij}\equiv E_j-E_i$. The density of fixed space charges is about 2.4×10^{13}, 7.6×10^{13}, and 2.4×10^{14} m^{-2}, respectively, for N_A equal to 10^{19}, 10^{20}, and 10^{21} m^{-3} when the Fermi level in the bulk is 44 meV below the conduction-band edge as assumed here. The values decrease slightly for the largest values of N_{sc}.

The optical absorption is readily calculated in the effective-mass approximation for the transmission-line configuration used by Kamgar *et al.*[8] We take the interaction term in the Hamiltonian in the form $\vec{\mathcal{E}}\cdot\vec{r}$, where $\vec{\mathcal{E}}$ is the far-infrared electric field, and write the effective-mass wave function as the product of an envelope function $f_i(z)$, a factor $\exp(i\vec{k}_j\cdot\vec{r})$ for motion parallel to the interface, and a periodic Bloch function.[12] Then the dipole matrix element contains a delta function in $\vec{k}_i-\vec{k}_j$ multiplied by

$$z_{ij}=\int_0^\infty f_i(z)zf_j(z)\,dz, \tag{1}$$

for sub-bands i and j arising from the same conduction-band valley, and is very small for sub-bands arising from different valleys. Values for

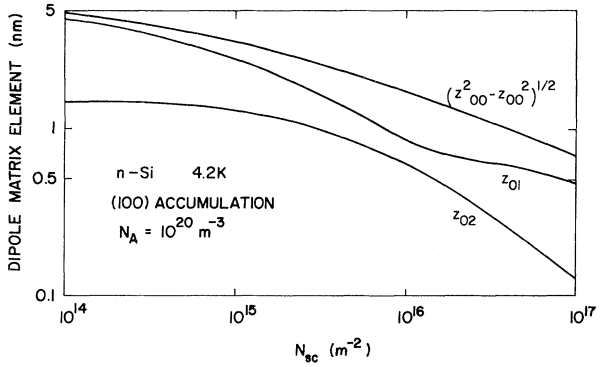

FIG. 2. Dipole matrix element versus total concentration of accumulation-layer space charges for optical transitions between the lowest sub-band and the first two excited sub-bands. The top curve gives the square root of the sums of the squares of the matrix elements connecting the lowest sub-band to all higher sub-bands in the effective-mass approximation; z_{ij} is defined in Eq. (1), and $(z^2)_{00}$ is the expectation value of z^2 for the lowest sub-band.

z_{01} and z_{02} are shown in Fig. 2.

The far-infrared electric field is assumed to be in the z direction and uniform across the transmission line. A small correction for the oxide layer has been ignored, as has the possible effect of higher-order modes.

The absorption coefficient for optical transitions between sub-bands i and j from the same valleys obtained with these assumptions is (in mks units)

$$\alpha_{ij}(E)=\frac{\pi e^2 N_{ji} z_{ij}^2 E S_{ij}(E)}{2\hbar\mu^{1/2}\epsilon^{3/2}d}, \qquad (2)$$

where ϵ is the permittivity, equal to 1.04×10^{-10} F/m for Si, μ is the permeability, equal to $4\pi\times10^{-7}$ H/m, d is the effective thickness of the sample, E is the photon energy, and $N_{ji}=N_i-N_j$ is the difference in electron concentrations of sub-bands i and j.

The shape function $S_{ij}(E)$ in Eq. (2) is a delta function centered at sub-band splitting E_{ij} in the simple effective-mass approximation, for which the wave-vector dependence of the energy is the same for all sub-bands arising from the same set of valleys.[12] Deviations from the effective-mass approximation, nonparabolicity, many-body effects, and lifetime broadening may all affect the form of $S_{ij}(E)$.

To estimate the magnitude of the absorption peak for transitions from the lowest sub-band to the first excited sub-band of the lowest valleys, we consider a case with 10^{16} electrons/m^2 in the lowest sub-band and essentially none in the first excited sub-band, use the matrix element z_{01} = 0.85 nm from Fig. 2, and estimate that at the absorption peak $ES_{01}(E)\approx 10$. We take the sample thickness d to be 200 μm and find that $\alpha_{01,\text{peak}}$ = 1.3 m^{-1}. No absolute absorption constants are given in Ref. 8, but the estimated value does not appear to be physically unreasonable.

The relative strength of the absorption to the first two excited sub-bands is predicted to be a rather strong function of the total space-charge concentration N_{sc}, as seen from the matrix elements in Fig. 2. The transitions to higher-lying sub-bands can be found from the relation $\sum z_{0i}^2 = (z^2)_{00}-z_{00}^2$. The square root of this quantity is also plotted in Fig. 2.

The sub-band splittings found experimentally cannot yet be compared directly with the calculations given here because the minority impurity concentration in the surface space-charge region of the sample used by Kamgar *et al.*[8] is not known, because there is some uncertainty in their threshold voltage, and because the calculated values do not include many-body effects such as exchange, correlation, or image terms. But the optical measurements greatly increase the chance of testing the assumptions underlying the calculations and of determining the magnitude of many-body effects. Availability of a tuned far-infrared laser would enhance the experimental possibilities.

I am indebted to A. Kamgar, J. F. Koch, G. Dorda, and P. Kneschaurek for valuable discussions and correspondence relating to their experiments, and to W. E. Howard and A. B. Fowler for valuable comments.

[1]C. B. Duke, Phys. Rev. 159, 632 (1967).
[2]G. A. Baraff and J. A. Appelbaum, Phys. Rev. B 5, 475 (1972).
[3]J. A. Pals, Philips Res. Rep., Suppl. No. 7, 1 (1972).
[4]D. C. Tsui, Phys. Rev. B 8, 2657 (1973).
[5]T. Hagiwara, O. Mizuno, and S. Tanaka, J. Phys. Soc. Jpn. 34, 973 (1973).
[6]R. Silbermann, G. Landwehr, and J. C. Thullier, in Proceedings of the Second International Conference on Solid Surfaces, Kyoto, Japan, 25–29 March 1974 (to be published).
[7]D. C. Tsui, G. Kaminsky, and P. H. Schmidt, Phys. Rev. B 9, 3524 (1974).
[8]A. Kamgar, P. Kneschaurek, G. Dorda, and J. F. Koch, Phys. Rev. Lett. 32, 1251 (1974).
[9]See, for example, R. A. Smith, *Semiconductors* (Cambridge Univ. Press, Cambridge, England, 1959), p. 91. We assume that only a single donor species is

present and that the impurity concentration is low enough that the donor level has not merged with the conduction band.

[10]See, for example, F. Stern, Phys. Rev. B 9, 4597 (1974), and 5, 4891 (1972), Appendix A.

[11]F. Stern, Phys. Rev. B 5, 4891 (1972).

[12]F. Stern and W. E. Howard, Phys. Rev. 163, 816 (1967).

Evidence for Ordered Layers of K^+ in KCP ($K_2[Pt(CN)_4]Cl_{0.3}\cdot 3H_2O$)

H. J. Deiseroth and H. Schulz
Max-Planck-Institut für Festkörperforschung, Stuttgart, Germany
(Received 2 July 1974)

We have redetermined the crystal structure of $K_2[Pt(CN)_4]Cl_{0.3}\cdot 3H_2O$. It crystallizes in space group $P4mm$, contrary to earlier assignments. The K^+ ions occupy ordered positions in layers with a periodicity of $c = 5.77$ Å which are perpendicular to the c axis. The same kind of superstructure was found for $K_2[Pt(CN)_4]Br_{0.3}\cdot 3H_2O$.

The compound $K_2[Pt(CN)_4]Cl_{0.3}\cdot 3H_2O$ (KCP) has recently attracted great attention because it is considered to be a one-dimensional conductor.[1-4] Its crystal structure is of fundamental importance for any interpretation of the physical properties and indispensable for theoretical considerations. Earlier determinations of the crystal structure of KCP were based on film methods only.[5] We have reinvestigated the crystal structure and found novel aspects of the atomic arrangements.[6]

With a single-crystal diffractometer (Syntex type $P2_1$) we have measured 529 symmetry-independent reflection intensities at room temperature. The average of the reflection intensities is much larger for (hkl) layers with $l = 2n$ than for $l = 2n+1$. Therefore, in the following, reflections with $l = 2n$ and $l = 2n+1$ are designated as main-structure and superstructure reflections, respectively. We obtained 290 main-structure and 55 superstructure reflections with $I > 3\sigma(I)$.[7]

With the use of these reflections and the structure model of Krogmann and Hausen[5] (KH model), R values, which are a measure of the agreement between observed and calculated structure factors, were calculated separately for main-structure and superstructure reflections:

$$R = \sum^{N} | |F_o| - |F_c| | / \sum^{N} |F_o|,$$

where F_o and F_c are the observed and the calculated structure factors, and N is the number of structure factors. The R value for main reflections is $R_1 = 0.03$, and for superstructure reflections, $R_2 = 0.54$. The low R_1 and the high R_2 values show that the KH model explains the main-structure but not the superstructure reflections.

In the KH model the Pt and K atoms have a periodicity parallel to the c axis of exactly $c/2$.[8] Therefore, these atoms do not contribute to the superstructure reflections. These reflections are generated only by C, N, and Cl atoms, and H_2O; see Fig. 1(a). We calculated a Patterson synthesis[9] using superstructure reflections only. The synthesis showed not only the maxima and minima required by the KH model but also a strong contribution of the K atoms. Furthermore, the data indicated that the K atoms occupy positions within one layer perpendicular to the c axis. This result contrasts with the KH model, where the K atoms are statistically distributed within two layers. The new K arrangement invalidates the previously assumed mirror plane perpendicular to the c axis. The tetragonal-space-group symmetry of the KH model ($P4/mmm$) is now reduced to $P4mm$. For this latter space group the four K atoms occupy the fourfold atomic position $4f$ in an ordered way.[10] Notice that the z coordinates of all atoms are no longer fixed. This superstructure model [Fig. 1(b)] was checked with structure refinements, for which again only the superstructure reflections were used. Our refinements converged at $R = 0.12$, which is a most favorable value considering the weak intensities. This R value agrees perfectly with the best theoretically possible R value, which follows from the standard deviations of the measured intensities. This is the proof that our superstructure is correct.

A difference Fourier synthesis using again only superstructure reflections did not show any contribution of Pt atoms. Furthermore, different